Advances in Bioceramics and Biotechnologies II.
Edited by Joanna M. McKittrick and Roger Narayan.

A COMPARISON ON THE STRUCTURAL AND MECHANICAL PROPERTIES OF UNTREATED AND DEPROTEINIZED NACRE

Maria I. Lopez[1], Po-Yu Chen[2], Joanna McKittrick[1,3], Marc A. Meyers[1,3]

[1] Materials Science and Engineering Program, University of California, San Diego, La Jolla, CA92093, USA
[2] Department of Materials Science and Engineering, National Tsing Hua University, Hsinchu 30013, ROC
[3] Department of Mechanical and Aerospace Engineering, University of California, San Diego, La Jolla, CA92093, USA

ABSTRACT

The contribution of the individual constituents of red abalone (*Haliotis rufescens*) to the strength of the nacre structure is investigated. Nacre sections were deproteinized to establish the contribution of the organic components. Tensile testing, scratch, and nanoindentation tests are performed on the isolated mineral constituent (deproteinized nacre) and the untreated nacre of red abalone shell. Specimens are characterized by scanning electron and atomic force microscopies to verify the deformation mechanisms. Results obtained from the isolated mineral validate the importance of the organic constituent, as the mechanical properties decline greatly when the organic component is removed. Scratch tests reveal the anisotropy of the material and the effects of the thick layers of protein (mesolayers) on the deformation behavior. This approach confirms the importance of the integrated structure to the overall mechanical behavior of nacre.

INTRODUCTION

In science and technology there is always a need for refining and improvements. Nature can provide excellent solutions to many of these difficulties. Understanding the property and structure relationship of biological materials by a materials science and engineering approach provides novel means of designing and processing synthetic materials.

In many cases, biological materials are a composite of biominerals and organics, which independently are quite weak [1]. Calcium carbonate, the mineral constituent of the abalone shell is quite brittle. However, when combined with an organic, nature creates a composite (nacre) that has a hierarchical, ordered structure with greatly improved mechanical properties.

The abalone nacre has various levels of organization ranging from the macro-structure to the nano-level [2]. The first level is the molecular structure of the chitin fibers that are the structural component of the intertile organic layers and of the atomic crystalline structure of the calcium carbonate phase, aragonite. The second level consists of the interface between the mineral tiles, which is composed of organic layers ~20 nm thick. In addition these interlayers are porous and allow mineral formations between adjacent tiles, known as mineral bridges [3,4]. The mineral bridges have a diameter of ~20-50 nm and a height of the interlayer. The third level consists of aragonite hexagonal tiles, with lateral dimensions of 8-10 μm and thickness of ~0.5 μm. These aragonite tiles are comprised of nanosized islands that arise due to the embedment of biopolymer [5,6]. The fourth level is the mesolayers, thick layers of biopolymer that are formed due to seasonal fluctuations [3,7-9]. The mesolayers are approximately ~200 μm thick and appear separating tile assemblages of approximately 0.1-0.5 mm thick. The fifth level of hierarchy is the entire structural geometry, including the hard outer calcitic layer, making it a two-layer armor system optimized for strength and toughness [10]. In this study, the primary focus will be on the second and third levels.

The structure-property relationship in abalone nacre has been intensively studied because it has the highest strength and toughness of any shells [1-36]. The arrangement of the parallel mineral tiles with the organic interface diminishes crack propagation as the crack has to travel along the organic layers creating a tortuous path, and accordingly the toughness and the work of fracture are enhanced. In addition, the structure is anisotropic which results in an orientation dependence of the mechanical properties. Moreover, because the hierarchical structure, different toughening mechanisms function at different levels suggesting the importance of understanding the mechanical properties at each level.

The objective of this investigation is to attain a better understanding of the structure-property relationship of the isolated constituents (e.g. isolated mineral and isolated organic component) in abalone nacre. When compared to the integrated (untreated) structure it can aid in determining the contributions of the different hierarchical levels and components. These results are significant to understand the important characteristics of abalone nacre to aid in improving the latest attempts to produce novel nacre-inspired materials.

MATERIALS AND METHODS

Deproteinization

Removal of all organic material from the nacre was performed by submerging the specimen in a basic solution. For the scratch and nanoindentation specimens, deproteinization was done by immersing it in a 5.2wt% sodium hypochlorite solution (NaClO) at 20 °C with constant mixing for a period of 12 days (where the solution was replaced daily). Due to the delicate nature of the nacre pucks for tensile testing, a less aggressive solution, 0.5N sodium hydroxide (NaOH) at 20°C for 10 days under constant, gentle shaking (Figure 1b) was utilized for the deproteinization of the nacre pucks for the tensile experiments. Deproteinization resulted in a separation of the sample where a mesolayer was present. The distance between mesolayers varies greatly between specimens; two mesolayers can be from 0.1μm to 1mm apart. Thus, when the removal of the organic constituent occurred the nacre pucks would separate along the mesolayers, yielding in samples of different thicknesses (0.1μm to 1mm thick).

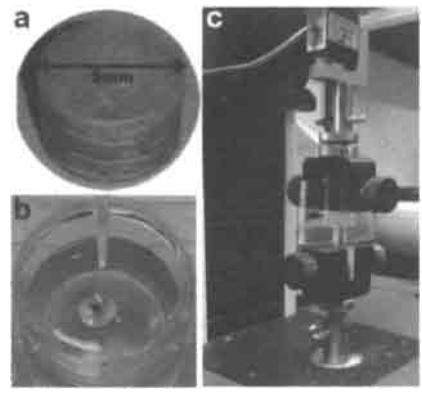

Figure 1: Experimental methods for tensile testing of deproteinized nacre pucks. a) Drilled puck specimen. b) Puck in deproteinizing solution. c) Mount setup for tensile testing.

Shell sectioning

Sectioning for tensile testing of deproteinized nacre was performed from two fresh abalone shells that were previously held and raised in an open water tank at the facility at the Scripps Institution of Oceanography, La Jolla, CA. The calcitic layer was removed via wet grinding, leaving only the nacreous layer. The samples were prepared by drilling cylindrical pucks of nacre, 5 mm in diameter, using a diamond coring drill (Figure 1a). Care was taken to

make lateral surfaces perpendicular to the concavity of the surface of the shell to ensure that the inner nacre layers are as parallel to the ends of the cylindrical specimen as possible. Specimens where then ground and polished to create a flat surface. The thickness of these specimens varied from 0.3-3 mm.

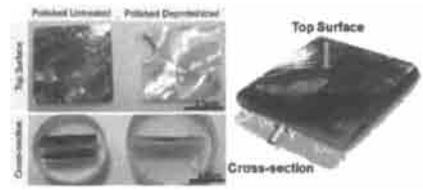

Figure 2: Nacre sectioning and mounting for scratch testing and nanoindentation.

For the scratch and nanoindentation specimens, nacre sections (3 cm x 3 cm x 0.3 cm) were cut using a diamond blade. Untreated specimens were directly mounted and polished. Deproteinized specimens were polished prior to and mounted after deproteinization. These specimens were prepared to be tested and characterized in two directions: top surface and in cross-section (Figure 2).

Mount Setup

For the tensile testing of the nacre pucks, a setup was created to decrease damage. Once the organic constituent is removed, the nacre becomes brittle and fragile. To reduce any pre-loading prior to testing, the pucks were mounted in an acrylic setup that allowed gripping and handling of the sample (Figure 1c). In this setup, the tensile load was applied perpendicular to the tiles.

Mechanical Testing

Tensile testing was performed in a tabletop desktop Instron 3342 system at strain rates of $10^{-2}s^{-1}$. Nanoscratching was performed utilizing a CSM Nano Scratch Tester specially suited to characterize practical adhesion failure of thin films and coatings, with a typical thickness below 800 nm. Samples were tested by applying a progressive load up to 1000 mN for specimens tested in cross-section, and by applying a progressive load up to 600 mN for specimens tested on the top-surface. The scratch length varied from 2-3 mm depending on the available surface area. At least six high-quality scratches were performed on each specimen. The fracture surfaces of all the specimens were gold-platinum coated and observed in a FEI SFEG Ultrahigh resolution scanning electron microscope (SEM). Nanoindentation was performed using a Hysitron nanoindentation system in various regions of the untreated and deproteinized nacre at loads ranging from 300 mN to 500 mN. Indented specimen was observed sequentially by atomic force microscope (AFM).

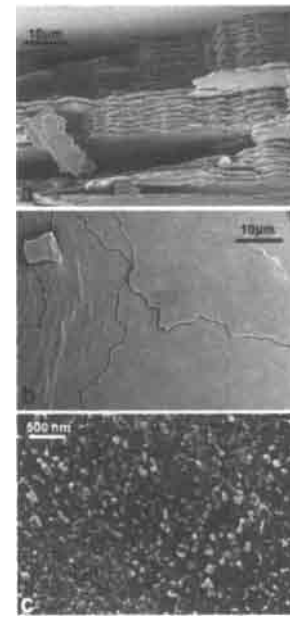

Figure 3: Imaging of deprotenized nacre pucks.
a) Cross-section showing the ~500 nm tiles.
b) 'Birds-eye-view' of fracture surface showing three different tile layers.
c) Nanoasperities covering the surface of the tiles.

RESULTS AND DISCUSSION

Imaging of Deproteinized Nacre

Figure 3 shows the cross-sectional view of the nacre after deproteinization. It can be noted that the mineral tiles remain completely intact retaining their ~500 nm thickness and shape (Figure 3a). Subsequent to tensile testing, the fracture surface of the puck was observed via SEM. Figure 3b show one of these surfaces (taken as a 'birds-eye-view'). Different tile layers are peeled off as the load is applied. Closer inspection of this top surface (Figure 3c) reveals nanoasperities that cover the entire tile face with a uniform distribution.

Previous experimentation done on demineralized nacre [36], reveal the structure of the isolated organic material as a porous one composed by a network of fibers. Comparing the imaging of the isolated organic material and the isolated mineral allow for interesting conclusions (Figure 4). The pores found within the organic interlayer are hypothesized to enable the formation of mineral bridges between adjacent tile layers. Because the imaging is done directly on the fracture surface, we can presume that some of the nanoasperities are actually fractured mineral bridges. The nanoasperities and the holes within the organic matrix sheet were measured. On average, the radius of the pores found in the organic interlayer is ~20 nm. In comparison, the average radius of the nanoasperities was found to be ~33 nm. This difference in diameter size might be due to the relaxation of the membrane as the material is demineralized. As the mineral is removed the pores in the organic interlayers are no longer under stress and thus reduce in size. Past investigations have focused in defining the role of these mineral bridges and how they correlate to the structure of the organic interface [29-32]. Mineral bridges appear as circular columns with diameters 25-55 nm [31, 32], while the pores exhibit a diameters 5-50 nm [33,34]. Current results show an average diameter than falls on the larger end of the previously reported values on the nanoasperities, however, pore diameter measurements fit well with previous results [28].

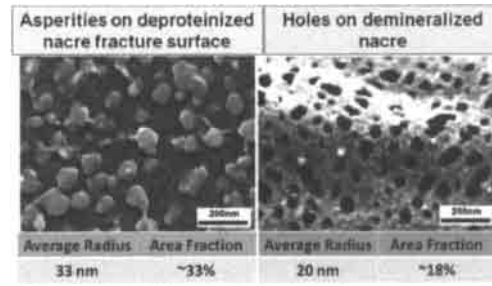

Figure 4: Comparison of the isolated organic material and the isolated mineral showing the differences in average diameter of asperities found on deproteinized nacre and the holes found on demineralized nacre.

However, it has been hypothesized that not all nanoasperities connect to form a mineral bridge. Previous studies suggest that in many cases the asperities only protrude [35]. The difference in the surface area covered by the nanoasperities and the area comprised by the holes in the membrane of the organic interlayer agrees with these previous results. Nanoasperities cover ~33% of the surface of the mineral tiles, compared to the area provided by the pores, which is estimated to be ~18%. Furthermore, Song and Bai [30] proposed that the average density distribution of mineral bridges vary – higher in the interior compared to the edges. In contrast, the current observations show a uniform distribution of nanoasperities on the surfaces of the tiles.

Tensile Tests of Deproteinized Nacre Pucks

Figure 5 shows the Weibull distribution of the deproteinized nacre pucks tested under tension with load perpendicular to layers. The 50% failure probability occurs at ~ 0.325 MPa, a low value, particularly when compared to the untreated nacre which shows a 50% failure probability at ~ 4.2 MPa.

Mineral bridges are believed to enhance stiffness, strength, and fracture toughness of the organic matrix by enhancing the crack extension pattern in nacre [29]. The theoretical strength of the mineral bridges is ~ 3.3 GPa [15]. If it is assumed that 18% of the surface area of each (approximating from the porous area in the organic intertile membrane) tile is covered by mineral bridges on samples 5 mm in diameter, the theoretical strength (3.3 GPa), far higher than what is measured. This can be due to several factors. There is likely an organic phase surrounding the mineral nanograins in the mineral bridges that deteriorated during the deproteinization process. Additionally, there is also the possibility that some of the mineral bridges were damaged or broken, previous to testing, lowering the strength values.

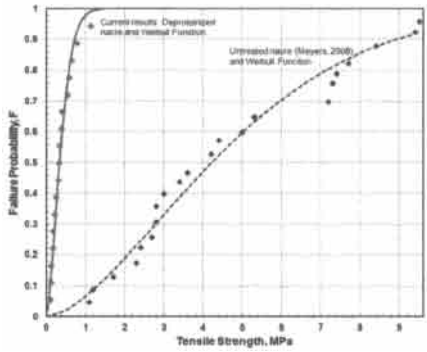

Figure 5: Weibull distribution of tensile strength perpendicular to layered structure of deproteinized nacre compared to results on whole nacre [15].

Nanoscratch Test

Figure 6 shows selected plots on the various sets of tests: a,b top surface untreated and deproteinized, respectively; b,c cross-section untreated and deproteinized, respectively. Interesting features can be noticed. When tested on the top surface, as expected, the deproteinized nacre fractures at lower loads than the untreated nacre; where major fractures began at the initial loading (3 mN) and fractured completely at loads lower than <100 mN. Force plots for this specimen do not show an explicit point of fracture and almost no resistance to scratching. In comparison the untreated nacre (tested on the top surface) exhibits a evident fracture limit, on average at ~27 mN. Furthermore, the anisotropic behavior can be noticed in the scratch tests. Compared to when tested on the top surface, when tested in the cross-section, the deproteinized nacre exhibited more of a resistance to scratching and demonstrated an explicit breaking point at ~120 mN. Additionally, when tested in cross-section, the untreated nacre does not show a precise frictional force limit; there is a gradual cracking which is more evident by SEM observations, discussed below. Furthermore, on untreated samples, mesolayers have an effect on the behavior and the frictional force. When tested in cross-section, mesolayers were encountered in various locations, when the indented tip meets a mesolayer, the scratch is deflected from its original path and follows through the mesolayer. It is also noticeable from the plot that the measured force

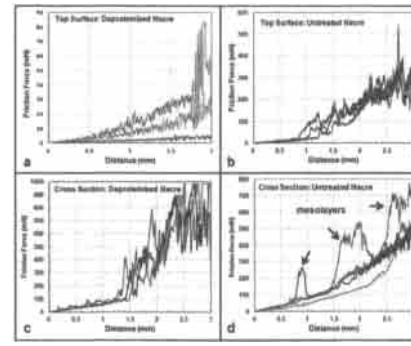

Figure 6: Microscratch force plots of: a) untreated nacre tested along the top surface, b) deproteinized nacre tested along the top surface, c) untreated nacre tested along the cross-section d) deproteinized nacre tested along the cross-section.

increases as the mesolayer is encountered giving an increased the resistance to motion, suggesting mesolayers add plowing friction.

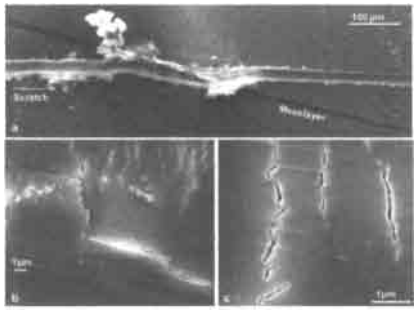

Figure 7: a) SEM micrograph of a scratch path encountering a mesolayer in untreated nacre. b) Fracture path in untreated nacre. c) Fracture path in deproteinized nacre.

When tested on the top surface, scratch profiles suggest that when the mineral is isolated there is very little resistance to fracture. This behavior corroborates similar behavior demonstrated by Bezares et al. [6], where nanoindentation was performed on heat-treated specimens where there was a loss in intra-tile protein. Heat-treated specimens appeared compacted, similar to heat-treated sand where grains begin to fuse together. However, in untreated specimens, the content of the organic component within the tiles that forms the 'nano-grain' structure the aragonite tiles in nacre, causing micro-crack deflection and crack blunting.

Moreover, there is an evident effect by all organic components in the material. The most evident feature of this is the mesolayers. Figure 7a shows an SEM micrograph of a scratch path encountering a mesolayer. As the scratch hits the mesolayer, the scratch path is deflected to follow the interface along the mesolayer. Furthermore, observations of the cross-section of tested untreated and deproteinized nacre show the impact of the organic interlayer. In the untreated nacre (Figure 7b) the crack propagates in a tortuous and step-wise; a much more complex path compared to that of deproteinized nacre. The crack is indeed deflected and arrested due to the successive combination of mineral and organic layers. The SEM image of the tested deproteinized nacre (Figure 7c) show that the crack growth precedes with a relatively unimpeded manner compared to the untreated nacre. Fractures occur through the tile and not necessarily following a predicted path. This difference in behavior again re-instates the importance of the organic component.

Nanoindentation experiments

Figure 8 shows AFM observations of an indentation on the center of the tile of untreated nacre. There is little, if any, crack propagation in untreated nacre when indented. For example in Figure 8a, the indent did not cause a crack, while in Figure 8b the indent created a crack. In Figure 8b, as the crack propagates, it reaches the edge it causing an aperture at the tile interface. Figure 9 shows the nanoindentation profile of deproteinized nacre. The surface of the deproteinized nacre is very different than that of the untreated nacre. The surface is rough and uneven. The tiles in nacre are known to contain embedment of organic material within the mineral [5]. With the deproteinization process, further than removing the organic interlayers,

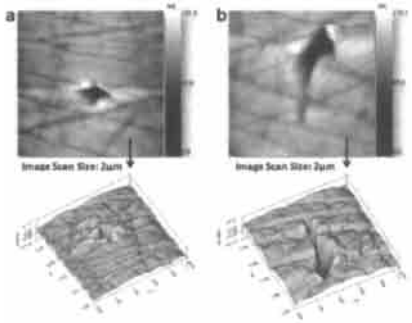

Figure 8: Nanoindentation profile of untreated nacre. a) Indentation contained within the tile, b) Indentation causes a crack to propagate which causes aperture at tile interface.

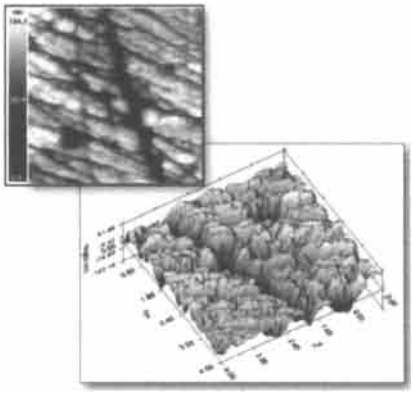

Figure 9: AFM observation of nanoindentation profile of deproteinized nacre. Extreme roughness and granular features conceal indent.

this embedded organic material within the mineral is also removed causing the gaps* in the surface of the tiles. The deproteinized nacre is extremely granular, thus when the diamond tip indents the surface, the indentation mark is concealed within the gaps. It is extremely difficult to observe any crack formation or propagation. These differences in nanoindentation profiles of the untreated nacre and deproteinized nacre agree with previous nanoindentation results by Bezares et al. [6]. Nanoindented untreated nacre showed pileups around edges, while heat-treated nacre was described as granular and loosely compacted. In this study, when the organic component is removed it also alters the structure of the mineral tiles, suggesting that in fact there is an embedment of organic constituent inside the tiles that impacts the mechanical properties.

CONCLUSIONS

The principal conclusions that can be drawn from the current research are:

1. From the mechanical testing of the deproteinized nacre we conclude that the behavior of the material, in particular the strength, is far below that of its theoretical strength. Even though the organic matrix accounts for only 10 vol% of nacre, when it is removed the strength is reduced by ~92% compared to whole nacre. This may be due to not only the removal of actual organic layers that have an effect of the weakening of the material, but also the removal of the organic material embedded within the mineral and/or bridges.
2. Some of the nanoasperities correspond to grains, and not mineral bridges. Distribution and density of the nanopores within the organic interlayer correspond to a better estimate of the number of mineral bridges.
3. When scratched on the top surface, deproteinized nacre fractures at a lower load and it does not show an explicit frictional force limit, compared to that of untreated nacre which exhibits an evident fracture limit (on average at ~27 mN). Furthermore, when scratched mesolayers (in untreated nacre) have an effect on the fracture behavior, adding a plowing force.
4. Scratch results also show the anisotropic behavior of nacre. In the scratch experiments nacre exhibits a higher resistance to failure when tested in cross-section (when the surface is along the tile layers) than from the top surface, in both, untreated and deproteinized specimens.
5. Nanoindentation results further reveal the effect of the loss of the organic constituent. Penetration in untreated nacre showed aperture at the tile interface while penetration in deproteinized nacre demonstrated the granular nature of the specimen due to the loss of the organic material.

ACKNOWLEDGEMENTS

This research is supported by National Science Foundation Grant DMR 1006931, NSF EAPSI Grant 1108531 and a Ford Foundation Pre-Doctoral Fellowship. Thanks go to Professor Duh, Yu-Chen, Hsien-Wei, Prof. JW Lee and his research group for help and access of

equipment at National Tsing Hua University and National Taipei University of Technology in Taiwan.

REFERENCES

1. Meyers MA, Chen PY, Lin AYM, Seki Y. Biological materials: structure and mechanical properties. Prog Mater Sci 2008;53:1-206.
2. Meyers MA, Chen PY, Lopez MI, Seki Y, Lin AY. Biological materials: a materials science approach. J. Mech Behav Biomed Mater 2011;4:626-57.
3. Schaffer TE, IonescuZanetti C, Proksch R, Fritz M, Walters DA, Almqvist N, et al. Does abalone nacre form by heteroepitaxial nucleation or by growth through mineral bridges? Chem Mater 1997;9:1731-40.
4. Meyers MA, Lim CT, Li A, Nizam BRH, Tan EPS, Seki Y, et al. The role of organic intertile layer in abalone nacre. Mat Sci Eng C-Mater 2009;29:2398-410.
5. Rousseau M, Lopez E, Stempfle P, Brendle M, Franke L, Guette A, et al. Multiscale structure of sheet nacre. Biomaterials 2005;26:6254-62.
6. Bezares J, Peng Z, Asaro RJ, Zhu Q. Macromolecular structure and viscoelastic response of the organic framework of nacre in *Haliotis rufescens*: a perspective and overview. Journal of Theoretical Applied Mechanics 2011;38:75-106.
7. Menig R, Meyers MH, Meyers MA, Vecchio KS. Quasi-static and dynamic mechanical response of *Haliotis rufescens* (abalone) shells. Acta Mater 2000;48:2383-98.
8. Lin A, Meyers MA. Growth and structure in abalone shell. Mat Sci Eng a-Struct 2005;390:27-41.
9. Su XW, Belcher AM, Zaremba CM, Morse DE, Stucky GD, Heuer AH. Structural and microstructural characterization of the growth lines and prismatic microarchitecture in red abalone shell and the microstructures of abalone "flat pearls". Chem Mater 2002;14:3106-17.
10. Cranford SW, Buehler MJ. Biomateriomics. Springer Durdrecht Heidelberg New York London 2012.
11. Zaremba CM, Belcher AM, Fritz M, Li YL, Mann S, Hansma PK. Critical transitions in the biofabrication of abalone shells and flat pearls. Chem Mater 1996;8:679-90.
12. Lin AYM, Meyers MA, Vecchio KS. Mechanical properties and structure of *Strombus gigas, Tridacna gigas*, and *Haliotis rufescens* sea shells: a comparative study. Mat Sci Eng C-Bio S 2006;26:1380-9.
13. Meyers MA, Lin AYM, Seki Y, Chen PY, Kad BK, Bodde S. Structural biological composites: an overview. Jom-Us 2006;58:35-41.
14. Lin AYM, Chen PY, Meyers MA. The growth of nacre in the abalone shell. Acta Biomater 2008;4:131-8.
15. Meyers MA, Lin AYM, Chen PY, Muyco J. Mechanical strength of abalone nacre: role of the soft organic layer. J Mech Behav Biomed 2008;1:76-85.
16. Kobayashi I, Samata T. Bivalve shell structure and organic matrix. Mat Sci Eng C-Bio S 2006;26:692-8.
17. Lin AYM, Meyers MA. Interfacial shear strength in abalone nacre. J Mech Behav Biomed 2009;2:607-12.
18. Sarikaya M, Gunnison, K. E., Yasrebi, M. and Aksay, J. A. Mechanical property – microstructural relationships in abalone shell. In Materials Synthesis Utilizing Biological Processes. Materials Research Society 1990;174:109-66.

19. Nakahara H, Kakei, M., and Bevelander, G. Electron microscopic and amino acid studies on the outer and inner shell layers of *Haliotis rufescens*. Venus Jpn J Malac 1982;41:33-46.
20. Sarikaya M, Aksay IA. Nacre of abalone shell: a natural multifunctional nanolaminated ceramicpolymer composite material. Results Probl Cell Differ 1992;19:1-26.
21. Nukala P.K.V.V., Simunovic S. A continuous damage random thresholds model for simulating the fracture behavior of nacre. Biomaterials 2005;26:6087-98.
22. Li XD, Xu ZH, Wang RZ. In situ observation of nanograin rotation and deformation in nacre. Nano Lett 2006;6:2301-4.
23. Currey JD, Kohn AJ. Fracture in crossed-lamellar structure of conus shells. J Mater Sci 1976;11:1615-23.
24. Currey JD. Mechanical-properties of mother of pearl in tension. P Roy Soc B-Biol Sci 1977;196:443.
25. Laraia VJ, Heuer AH. Novel composite microstructure and mechanical-behavior of mollusk shell. J. Am Ceram Soc 1989;72:2177-9.
26. Barthelat F, Espinosa HD. An experimental investigation of deformation and fracture of nacre mother of pearl. Exp Mech 2007;47:311-24.
27. Barthelat F, Tang H, Zavattieri PD, Li CM, Espinosa HD. On the mechanics of mother-of-pearl: A key feature in the material hierarchical structure. J Mech Phys Solids 2007;55:306-37.
28. Tang H, Barthelat F, Espinosa HD. An elasto-viscoplastic interface model for investigating the constitutive behavior of nacre. J Mech Phys Solids 2007;55:1410-38.
29. Song F, Bai YL. Mineral bridges of nacre and its effects. Acta Mech Sinica 2001;17:251-7.
30. Song F, Zhang XH, Bai YL. Microstructure and characteristics in the organic matrix layers of nacre. J. Mater Res 2002;17:1567-70.
31. Song, F., Soh, A. K. and Bai, Y. L. Structural and mechanical properties of the organic matrix layers of nacre. Biomaterials 2004; 24, 3623-3631
32. Gries K, Kroger R, Kubel C, Fritz M, Rosenauer A. Investigations of voids in the aragonite platelets of nacre. Acta Biomater 2009;5:3038-44.
33. Bezares J, Asaro RJ, Hawley M. Macromolecular structure of the organic framework of nacre in *Haliotis rufescens*: Implications for growth and mechanical behavior. J Struct Biol 2008;163:61-75.
34. Bezares J, Asaro RJ, Hawley M. Macromolecular structure of the organic framework of nacre in *Haliotis rufescens*: Implications for mechanical response. J Struct Biol 2010;170:484-500.
35. Checa AG, Cartwright JH, Willinger MG. Mineral bridges in nacre. J Struct Biol 2011;176:330-9.
36. Lopez MI, Meza-Martinez PE, Meyers MA, Organic Interlamellar layers, Mesolayers, and Mineral Nanobridges: Contribution to Strength in Abalone (Haliotis rufecens) Nacre. Acta Biomaterialia (Submitted, 2013)